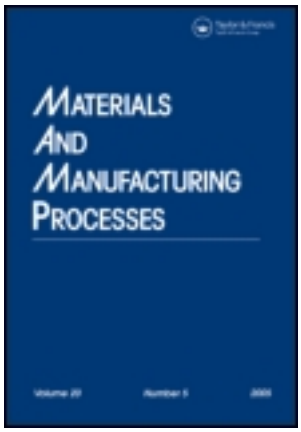

Materials and Manufacturing Processes
Publication details, including instructions for authors and subscription information:
http://www.tandfonline.com/loi/lmmp20

Device Simulation-Based Multiobjective Evolutionary Algorithm for Process Optimization of Semiconductor Solar Cells

Yiming Li [a], Yu-Yu Chen [a], Chieh-Yang Chen [a], Cheng-Han Shen [a], Hui-Wen Cheng [a], I-Hsiu Lo [a] & Chun-Nan Chen [b]

[a] Parallel and Scientific Computing Laboratory, Department of Electrical and Computer Engineering, National Chiao Tung University, Hsinchu, Taiwan

[b] Quantum Engineering Laboratory, Department of Physics, Tamkang University, Taipei, Taiwan

Published online: 08 Jul 2013.

To cite this article: Yiming Li, Yu-Yu Chen, Chieh-Yang Chen, Cheng-Han Shen, Hui-Wen Cheng, I-Hsiu Lo & Chun-Nan Chen (2013) Device Simulation-Based Multiobjective Evolutionary Algorithm for Process Optimization of Semiconductor Solar Cells, Materials and Manufacturing Processes, 28:7, 761-767, DOI: 10.1080/10426914.2013.792433

To link to this article: http://dx.doi.org/10.1080/10426914.2013.792433

Materials and Manufacturing Processes, 28: 761–767, 2013

ISSN: 1042-6914 print/1532-2475 online
DOI: 10.1080/10426914.2013.792433

Taylor & Francis
Taylor & Francis Group

Device Simulation–Based Multiobjective Evolutionary Algorithm for Process Optimization of Semiconductor Solar Cells

Yiming Li[1], Yu-Yu Chen[1], Chieh-Yang Chen[1], Cheng-Han Shen[1], Hui-Wen Cheng[1], I-Hsiu Lo[1], and Chun-Nan Chen[2]

[1]*Parallel and Scientific Computing Laboratory, Department of Electrical and Computer Engineering, National Chiao Tung University, Hsinchu, Taiwan*
[2]*Quantum Engineering Laboratory, Department of Physics, Tamkang University, Taipei, Taiwan*

This article implements for the first time a numerical semiconductor device simulation-based multiobjective evolutionary algorithm (MOEA) for the characteristic optimization of amorphous silicon thin-film solar cells, based upon a unified optimization framework (UOF). To calculate the device's characteristic, a set of coupled solar cell transport equations consisting of the Poisson equation, the electron-hole current continuity equations, and the photo-generation model is solved numerically. Electrical characteristics, the short-circuited current, the open-circuited voltage, and the conversion efficiency are calculated to analyze the properties of the explored solar cells. The aforementioned device simulation results are used to evaluate the fitness score and access the evolutionary quality of designing parameters via the implemented non-dominating sorting genetic algorithm (NSGA-II) in the UOF. Notably, designing parameters including the material and structural parameters, and the doping concentrations are simultaneously optimized for the explored solar cells. The simulation-based MOEA methodology is useful in optimal structure design and manufacturing of semiconductor solar cells.

Keywords Amorphous silicon; Design optimization; Material and structural parameters; MOEA; Multiobjective; Simulation-based evolutionary method; Thin film solar.

Introduction

Solar energy is zero-emission and renewable, so semiconductor devices, in particular, silicon-based solar cells, used for converting sunlight to electrical power have been more attractive in recent years [1–6]. As the energy demand is growing, it is necessary for us to decrease the fabrication cost of semiconductor solar cells and improve the energy conversion efficiency (η) for the potential of reducing fossil fuel consumption and more electrical power generation potentially. Currently, the materials of crystalline silicon (c-Si), polycrystalline silicon (poly-Si), and amorphous silicon (a-Si) have been of great interest for manufacturing of silicon-based solar cells [7]. Most of optimal designs of thin-film Si solar cells for pursuing the higher conversion efficiency are mainly achieved empirically. Genetic algorithm (GA) is a population-based global search optimization method based on the mechanics of natural selection, and often considered as the most famous branch in evolutionary algorithms [8, 9]. Nowadays, the GA with the appropriate elitist policy can guarantee the global best solution acquirement theoretically and generally can provide many near-optimal selections of the problem varying from semiconductor nanostructures to electronic circuits [10–20]. Recently, the GA was adopted for solving single objective optimization problems in electrical characteristic design of solar cells [21]. However, diverse solar cell engineering designing problems are high complexity and there are usually with multiple constraints and designing requirements. Mathematically, a solar cell designing problem can be modeled as a multiobjective optimization problem. Optimizing the parameters of the solar cell's multiobjective optimization problem by using the multiobjective evolutionary algorithm (MOEA) will be interesting for the academic and industrial domains [22–27].

In this work, based upon a unified optimization framework (UOF) [28], a device simulation-based MOEA is proposed for a-Si thin-film solar cell design optimization, where the nondominating sorting genetic algorithm (NSGA-II) [24, 25] is implemented for its good performance. To calculate the device characteristic, a set of coupled solar cell transport equations consisting of the Poisson equation, electron-hole current continuity equations, and the photo-generation model is solved numerically [29–33]. The results of device simulation including the short-circuited current (I_{sc}), the open-circuited voltage (V_{oc}), and the conversion efficiency (η) are used for the fitness calculation; consequently, the quality of designing parameters is evaluated via the NSGA-II. The iteration of evolutionary process is terminated when the results meet the prescribed targets. The optimization approach presented in this work allows us to at the same time optimize the electrical characteristics, for a *p-i-n* structure of a-Si thin-film solar cell

Received March 16, 2013; Accepted March 16, 2013
Address correspondence to Yiming Li, Parallel and Scientific Computing Laboratory, Department of Electrical and Computer Engineering, National Chiao Tung University, 1001 Ta-Hsueh Road, Hsinchu 300, Taiwan; E-mail: ymli@faculty.nctu.edu.tw

with original efficiency of 5.68%, $\eta = 8.1\%$ is obtained successfully. This study shows practical application in solar cell characterization and structure optimal design.

In the next section, we describe the parameters of examined a-Si thin-film solar cell to be optimized briefly. We then introduce the device simulation-based MOEA optimization technique on the UOF. In Section 4, we will discuss the optimization results in terms of computational and electrical meanings in detail. We finally draw the conclusion and list future work.

The solar cell and the optimization technique

For real-world application of solar energy, it is important to decrease the manufacturing cost and increase the efficiency of power conversion [7]. In order to make efficient photo converters of *p-n* junctions with high collection efficiency, it is necessary for us to equip the diffusion length of minority carriers which exceeds typical absorption depths [1, 2]. However, c-Si is very high-priced in production; it has been of great interest to consider other photovoltaic materials of less requiring the quality of silicon which can be processed relatively low in price. At present, a-Si has been identified as one of the best materials with the advantage mentioned above. This thin film material is usually produced by physical or chemical deposition techniques which can be applied to large areas and throughputs [1, 2, 7].

The basic configuration of a-Si solar cell is a *p-i-n* structure, as shown in Fig. 1. The silver and Si_3N_4 are the front contact metal and antireflection layer [3–5]. For doped a-Si, the diffusion length is very short physically, so we consider a central undoped, lightly doped, or intrinsic region to extend its thickness so that photons could be absorbed effectively. The material and structural parameters to be optimized are explained in Fig. 1. The feasible numeric ranges of the parameters are listed in Table 1 according to device physics of solar cell. In order to estimate the electrical characteristics of the studied solar cells, three governing equations which include the Poisson equation and the electron-hole current continuity equations in semiconductor are solved self-consistently [28–32]. They indicate that the number of carriers is conserved and the electrostatic potential due to the carrier charges obeys Poisson's equation. In the electron-hole current continuity equations, the generation rate is an electronic excitation event which increases the number of free carriers available to carry charge and the recombination rate is an electronic relaxation event which reduces the number of free carriers. For the studied a-Si thin-film solar cells, the most important form of generation G_n and G_p is optical generation G^{opt}. The G^{opt} is calculated from the optical part, where a set of Maxwell's equations is solved [1, 2].

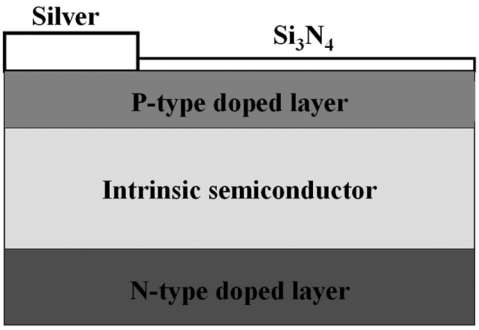

Parameters to be optimized of the studied *p-i-n* solar cell

- Thickness of silver: *Front Contact Thickness* (μm)
- Thickness of the anti-reflection layer Si_3N_4: *Front Arc Thickness* (μm)
- Thickness of the all semiconductors: *Substrate Thickness* (μm)
- Doping concentration of the *p*-layer: *Front Doping Concentration* (cm^{-3})
- Dopant depth of the p-layer: *Front Doping Depth* (μm)
- Doping concentration of the *n*-layer: *Back Doping Concentration* (cm^{-3})
- Dopant depth of the n-layer: *Back Doping Depth* (μm)

Figure 1.—Plot of the optimized a-Si solar cell with the *p-i-n* structure. The parameters to be optimized include the layer's thickness and doping profile of each layer.

Notably, in the approach by using GA for solar cell optimization problems, weighting function is the most commonly used skill to construct the function, but the critical issue is that the function cannot perfectly describe the original design problems, and there is no standard rule to determine the weightings [21]. Actually, solar cell design problems belong to multiobjective optimization problems (MOPs). Such problems have more than one objective function discussed above and thus usually have many optimal solutions, known as Pareto optimal solutions. These solutions can help designers verify the relationships among various objectives, and provide several options for the posteriors decision making. In other words, formulating the design problems to MOPs is intuitive and much easier than typical GA approaches, and the optimal solutions of the problems involve more information. Many algorithms have been proposed to solve MOPs [8, 9, 22–26]. Because the population-based parallel process of evolutionary computing techniques has consistency to the property of MOPs (multiple optimum solutions achievement), MOEAs have received attentions and become the most popular approach to solve MOPs. The general scenario of an MOEA is that randomly initializes the population (the set of possible designs) in the search space, and then evolves it generation by generation until the stop criterions are reached. In the above flow, the MOEA must achieve the fitness values of each design in the

Table 1.—Feasible numeric range of the parameters to be optimized.

Parameters to be optimized	Feasible numeric range
Substrate Thickness (μm)	0.50–1.00
Front Contact Thickness (μm)	0.05–0.3
Front Arc Thickness (μm)	0.02–0.2
Back Doping Concentration (cm^{-3})	1×10^{18}–1×10^{20}
Back Doping Depth (μm)	0.01–0.30
Front Doping Concentration (cm^{-3})	1×10^{18}–1×10^{20}
Front Doping Depth (μm)	0.001–0.1

population every generation. The common method to obtain the values, which is known as simulation-based approach, is by calling external computationally expensive numerical semiconductor device simulation programs to implement the exact evaluations. Note that, the proposed UOF can be used by GA and MOEA. GA is a classical algorithm while MOEA is similar but introducing multiobjective concept; both are tested and compared in the solar cell design problem. The MOEA algorithm improves one of the disadvantages of GA: the weighting value of fitness calculation. While fitness is a value used to compare each individual, it will be simple if there is only one objective. If there are many objectives, the calculated value of each objective is multiplied weighting and summed to obtain the fitness. The weighting's value could be calibrated empirically, which is a time-consuming task, and actually it can only find the best point of a fitting line generated by the weighting products sum. Because weighting products sum fitness is hard to find best characteristic of each objective simultaneously, MOEA algorithm has no weighting and find best characteristic of each objective simultaneously. When one objective problem, it is significant that largest value is the best (or "dominant"). The dominant concept is used in MOEA, the objective values of dominant solutions form a "pareto front" curve for any arbitrary two objective values in two-dimensional (2D); similarly, it can also form a surface in three dimensions.

The solar cell design problem is solved by using MOEA which is implemented on the UOF together with the numerical semiconductor device simulation [27–32]. Note that the UOF is an objective-oriented optimization framework for general optimization problem. A specific MOEA, the NSGA-II is chosen because of its reliability and parameterless characteristic [24–25]. The optimization technique is used to optimize the performance of a-Si thin film solar cells. There are two main components of the UOF which is the Problem and Solver. For each component, it is designed from the high-level code to can be reused and fast to response. In brief, the UOF is a basic interface to bridge that defining a problem and fast solving the problem by a variety of methods. The design of UOF has a robust advantage that the numerical simulation programs as well as the optimization solvers can be changed and used easily for other applications. In this work, we use 2D numerical semiconductor device simulation to simulate the optical and electrical properties of the a-Si *p-i-n* solar cell, such as the optical generation rate, the electric field, and the electron-hole densities; consequently, the corresponding electrical V_{oc}, J_{sc}, and η of the solar cell are calculated. To achieve the aforementioned specifications, we set the V_{oc}, J_{sc}, and η as three objective functions to be maximized, where all parameters have their constraints and feasible numeric ranges, as listed in Table 1. The adopted solver MOEA optimizes the studied solar cell, which includes four operations, evaluation, selection, crossover, and mutation; and the evaluation and fitness assign are modified owing to the multiobjectives.

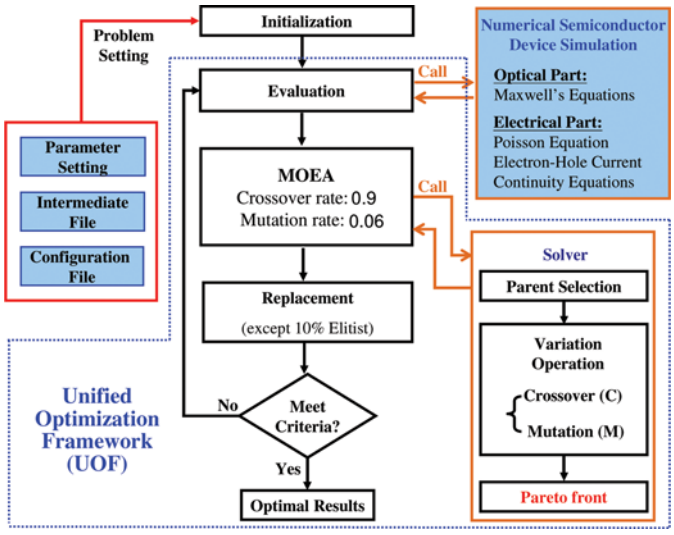

FIGURE 2.—The proposed optimization technique based upon UOF to optimize the electrical characteristics and conversion efficiency of the tested a-Si solar cell with the simulation-based MOEA. Empirically, the crossover rate is 0.9, and the mutation rate is 0.06. The mutation rate is smaller than the crossover rate; it implies that only few populations are required to mutate. The computing platform used in this study has the processor of a 3.1 GHz Xeon processor (4 CPUs) and the main memory of 8 GB SRAM, which is running with a Linux kernel of CentOS release 5.8. The computational time to run a solar cell design optimization takes more than 12 hours, where the time for each numerical simulation of the solar cell's optical and electrical characteristics is 1,200 sec with all evolutionary parameters (color figure available online).

The whole optimization flow of the technique is shown in Fig. 2. In the mask and parameter setting files, we define the given structure and the parameters to be optimized of the a-Si solar cell. Then, the population, which means the group of parameter configurations, is initially generated randomly or by engineering experiences. After the initial population established, all individuals in the population are evaluated by numerical semiconductor device simulation program to obtain the goal characteristic. We further assign each population the fitness value, which is determined by the optimization method. According to GA, we generate next iteration from last population. The parents are selected by random competition; and individuals which have better fitness value have more probability and the weak remain in small proportion. The variation operation contains two mechanisms: crossover and mutation. Crossover is used as the first operator applied on the parents. One parent will inherit the genes (parameters in the array) of an offspring from beginning to split point (randomly determined afresh in each offspring production), where the other takes the rest. By using the second operator, mutation, we can select two genes in one individual in a statistically sound way (i.e., totally random approach) and exchange them under the probability of mutation rate. Finally, except the best 10% individuals in the old population, which are called elitists, the offspring after variation operators will act in

place of the rest of the old population. Iteratively, a new population established and next generation of evolution starts from evaluation step until the stop criteria are met.

Results and discussion

With the parameters listed in Table 1, both the population size and the maximum generation are 100 in the tested solar cells. Our target is to maximize the device's voltage, current density, as well as its efficiency for advanced energy harvesting applications. To estimate the electrical characteristics of the a-Si solar cell we use the simulated reflectance spectra. The property of optical system affects seriously the short-circuit current density and the conversion efficiency of a solar cell. So the short-circuit current density and the open-circuit voltage of the solar cell are calculated under the standard AM1.5 global spectrum from its current and voltage (I-V) characteristics. Then, the solar cell's conversion efficiency deduced from V_{oc} and I_{sc} is given by

$$\eta = \frac{P_{\max}}{I_{sc}V_{OC}}\frac{I_{SC}V_{OC}}{P_I} = \frac{P_{\max}}{P_I} \times 100\%, \quad (1)$$

where P_I designates the incident power ($P_I = 0.1\,\mathrm{W/cm^2}$ under illumination AM 1.5 G) and P_{max} is the largest electrical power the solar cell can deliver. First, we give a proper range of the parameters of the structure to optimize the efficiency. The results of our optimization are shown in Fig. 3, where the results obtained by using GA and MOEA are compared. The original design is 5.68%, as shown in Fig. 3, both the GA and MOEA show significant improvement in the conversion efficiency.

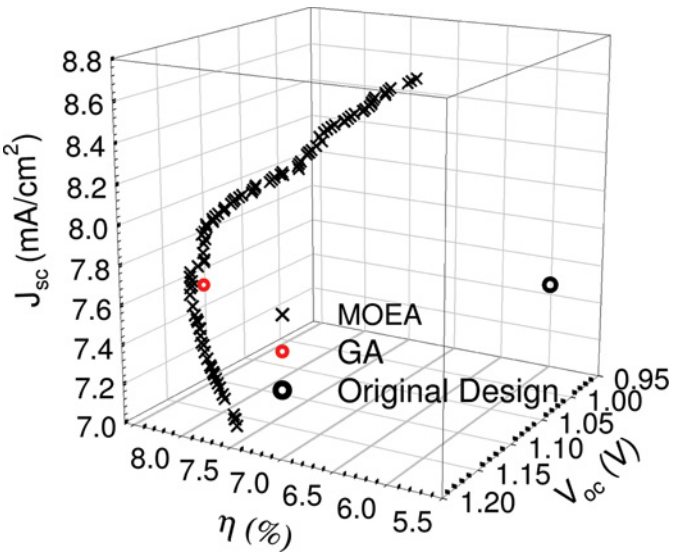

Figure 3.—The key results of MOEA implemented in this work as well as the result of GA show that the solution of our optimization is better than that of GA and can discover the optimal solutions in overall decision space (color figure available online).

Nevertheless, the solutions of the MOEA imply more information within the engineering limitation of the solar cell, compared with the result of GA. The efficiency of MOEA optimized result is about 41.3 percent improvement from the default efficiency 5.68%. In addition, we can see that the '*Front Doping Depth*' is the largest value and the '*Back Doping Depth*' is the smallest value, which shows the fact that higher '*Front Doping Depth*' and the lower '*Back Doping Depth*' are the superior design strategy for a-Si thin film solar cells. From semiconductor device physics, the designs using both the GA and MOEA show that the p-layer is much thinner than the n-layer, which is accommodated to typical design methodology because the diffusion length of hole is much shorter than the diffusion length of electron. Furthermore, we discover that the thickness of antireflection layer for decreasing the sunlight reflectance might be lower than 50 nm in our case. Second, we further apply different parameter range but same structure to maximize the V_{oc} and I_{sc}, respectively. The results show that the '*Front Doping Concentration*' should be high for both improving V_{oc} and I_{sc}.

By considering the conversion efficiency as the only objective to be maximized, the GA optimized conversion efficiency $\eta \approx 8.0\%$, which is close to the conversion efficiency by the MOEA, as shown in Fig. 3. In this test, the MOEA optimized results are $\eta = 8.1\%$, $I_{sc} = 7.76\,\mathrm{mA/cm^2}$, and $V_{oc} = 1.1732\,\mathrm{V}$. However, as listed in Table 2, if we set the requirements: $\eta > 8\%$, $I_{sc} > 8\,\mathrm{mA/cm^2}$, and $V_{oc} > 1.1\,\mathrm{V}$, from the results of MOEA, we can find four possible solutions, MOEA Sol. 1–MOEA Sol. 4, among the results of MOEA. However, the GA only optimizes each requirement one by one. The results, GA Sol. 1–GA Sol. 3, by the GA approach achieve the aforementioned specification separately, but the GA cannot optimize the requirements: $\eta > 8\%$, $I_{sc} > 8\,\mathrm{mA/cm^2}$, and $V_{oc} > 1.1\,\mathrm{V}$ at the same time.

We further compare the results between the MOEA and GA in terms of the pairwised relationship among the aforementioned electrical specifications. Figure 4 shows a relationship between the achieved V_{oc} and η. When the device's voltage is below 1.14 V, we can increase the device's efficiency along with the increase of operation voltage at the same time. They possess a positive correlation. However, if the voltage of a-Si solar cell is larger than 1.7 V, the efficiency is saturated and cannot be increased any more, where a turnaround point appears. The MOEA's result improves the GA-found efficiency, as shown in Fig. 4, the new found 8.1%-efficiency by the MOEA is better than the GA's results.

Figure 5 shows the plot of J_{sc} vs. V_{oc}. The current density drops significantly when the operation voltage is larger than 1.14 V. Their relationship is almost negative correlation, but the optimal I-V point found by MOEA and GA is very similar. The results of the current density

TABLE 2.——The optimized results of a-Si solar cell for the requirements: $\eta > 8\%$, $I_{sc} > 8\,mA/cm^2$, and $V_{oc} > 1.1\,V$. There are four possible MOEA solutions that can achieve the requirements. The GA can achieve each requirement separately.

	Substrate thickness (μm)	*Front contact thickness* (μm)	*Front arc thickness* (μm)	*Back doping concentration* (cm^{-3})	*Back doping depth* (μm)	*Front doping concentration* (cm^{-3})	*Front doping depth* (μm)	η (%)	V_{oc} (V)	J_{sc} (mA/cm^{-2})
MOEA Sol.1	0.6549	0.1665	0.051	5.296E19	0.2021	2.511E19	0.063	8.04	1.1455	8.01
MOEA Sol.2	0.7248	0.1953	0.050	5.685E19	0.2101	2.675E19	0.079	8.02	1.1409	8.02
MOEA Sol.3	0.7254	0.1956	0.050	5.658E19	0.2100	2.662E19	0.078	8.02	1.1398	8.03
MOEA Sol.4	0.6519	0.1676	0.051	5.334E19	0.2023	2.554E19	0.063	8.05	1.1480	8.00
GA Sol.1	0.6500	0.3000	0.040	4.800E19	0.2000	6.800E19	0.092	8.00	1.1590	7.7
GA Sol.2	0.5000	0.2000	0.050	7.400E19	0.1000	9.500E19	0.100	7.27	1.1687	6.95
GA Sol.3	1.0000	0.0500	0.050	4.100E19	0.1000	4.250E19	0.060	6.79	0.9841	8.64

vs. the efficiency on MOEA and GA are shown in Fig. 6. It implies that the when the current density is smaller then $8.1\,mA/cm^2$, the relationship is positive correlation between the current density and the efficiency. When the current density is larger then $8.1\,mA/cm^2$, the relationship behaves negative correlation between the current density and the efficiency. The MOEA's result improves the GA-found efficiency, as shown in Fig. 6, the new found 8.1%-efficiency by the MOEA which maintains a relatively higher level of the current density is better than the GA's results. The computational observation discussed above enable us to apply the optimized results of the MOEA to estimate the a-Si material and *p-i-n* structural limitations of the studied solar cell, which is beyond the scope of GA.

Notably, as shown in Figs. 4–6, the results of GA could not get better solution on each domain. It is obviously that the GA can deal with single-target problems; for a multiobjective problem, GA requires a proper cost function with empirically turned weighting coefficients. In contrast to the GA, the MOEA can solve the multiobjective solar cell problem by optimizing the three objective functions at the same time, which implies that the MOEA can even get the better solutions on three directions. To verify the manufacturability of the MOEA optimized material and structural parameters, we further fabricate a-Si sample based on the fabrication line of silicon solar cell. The flow chart of the fabrication process for solar cell follows our recent work in [4]. After the structure fabrication process, the post processing of the cell is finished under AM1.5 G conditions. The post processing includes electrode formation by standard screen printing method and the cell characterization to obtain the V_{oc}, J_{sc}, and η. The measured conversion efficiency of 9.6% is even better than the optimized result (about 8.0%) from the proposed MOEA. The difference between the measured (9.6%) and optimized (8.0%) efficiencies can be attributed to the different design of reflectance layer of the fabricated sample. In this work, the reflectance layer of Si_3N_4 is a thin film layer which is different from the fabricated sample. The optimization and sample fabrication show that the numerical semiconductor device simulation-based MOEA methodology is promising for solar cell design and manufacturing.

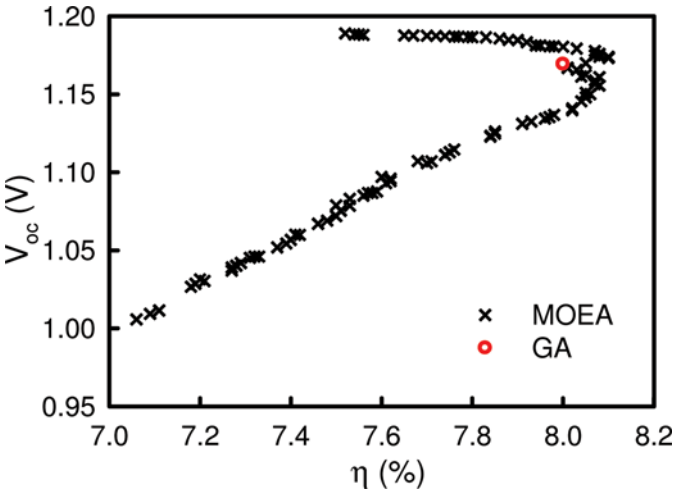

FIGURE 4.—The results of the open-circuit voltage vs. the conversion efficiency on MOEA and simple GA. A relationship between the V_{oc} and η is further examined; under a level of open-circuit voltage, it is possible for us to increase the V_{oc} and η, simultaneously. Notably, the η reaches its maximum when $V_{oc} > 1.7\,V$ (color figure available online).

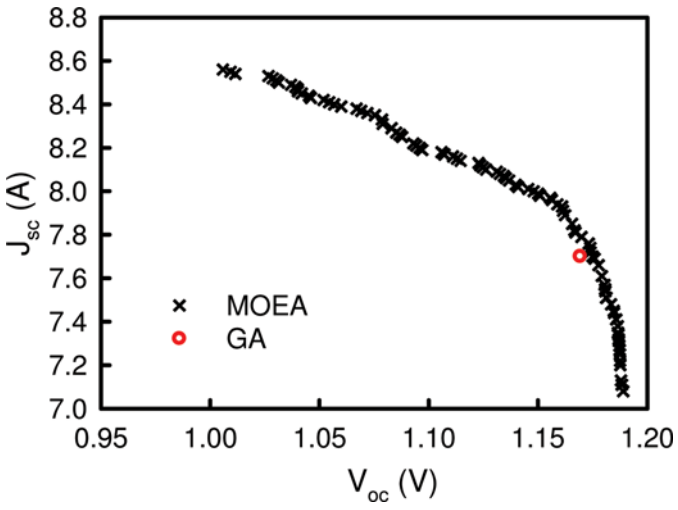

FIGURE 5.—The results of the current density versus the voltage on MOEA and simple GA which indicate the I-V relationship is almost negative correlation (color figure available online).

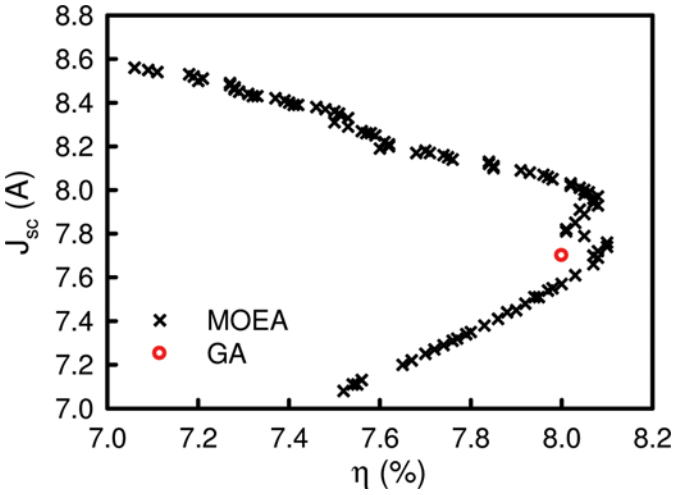

FIGURE 6.—The results of the current density vs. the efficiency on MOEA and GA. It indicates that the when under a level of the current density (about 7.8 mA/cm^2–8.1 mA/cm^2), the relationship is positive correlation between the J_{sc} and η. When the current density is larger then 8.1 mA/cm^2, the relationship turns to negative correlation (color figure available online).

CONCLUSIONS

In this study, based upon a unified optimization framework, a numerical semiconductor device simulation-based MOEA is implemented for amorphous silicon thin-film solar cell optimization problem and achieves superior results. By simultaneously maximizing the open-circuit voltage, short-circuit current density, and conversion efficiency, the results of MOEA optimization technique, not only enable us to design the tested a-Si *p-i-n* solar cells, but also show interesting and potential designing parameters, compared with the results of GA and the original design. The approach of simulation-based MOEA presented in this work is an alternate optimization method by using statistical Taguchi quality design [34]. Notably, the efficiency of 8.0% optimized from the MOEA methodology is significantly increased from the original efficiency of 5.68%. This simulation-based MOEA methodology running on the UOF can be used in solar cell characterization and optimal structure design. Consequently, it will benefit the manufacturing of semiconductor solar cells. We are currently applying this optimization technique to design semiconductor solar cells with embedded array of quantum dots.

Notably, directly and iteratively solving the Maxwell's equations and drift-diffusion equations for the optical property and transport characteristic of the solar cell would be very time consuming and highly computing intensive. Meta-modeling approaches with considering the recent advents of the EvoNN and BioGP algorithms [35–37] could provide a cost-efficient evolutionary way in solar cell design optimization.

ACKNOWLEDGMENTS

This work was supported in part by the National Science Council, Taiwan, under Contract Nos. NSC-100-2221-E-009-018 and NSC-101-2221-E-009-092.

REFERENCES

1. Sze, S.M. *Physics of Semiconductor Devices*; Wiley-Interscience: New York, 1981.
2. Nelson, J. *The Physics of Solar Cells*; Imperial College Press: London, **2003**.
3. Li, Y.; Lee, M.-Y.; Cheng, H.-W.; Lu, Z.-L. 3D imulation of morphological effect on reflectance of Si_3N_4 sub-wavelength structures for silicon solar cells. *Nanoscale Research Letters* **2012**, *7*, 196.
4. Sahoo, K.C.; Li, Y.; Chang, E.Y. Shape effect of silicon nitride sub-wavelength structure on reflectance for solar cell application. *IEEE Transactions on Electron Devices* **2010**, *57*, 2427–2433.
5. Sahoo, K.C.; Li, Y.; Chang, E.Y. Numerical calculation of the reflectance of sub-wavelength structures on silicon nitride for solar cell application. *Computer Physics Communications* **2009**, *180*, 1721–1729.
6. Hu, W.; Budiman, M.F.; Igarashi, M.; Lee, M.-Y.; Li, Y.; Samukawa, S. In-plane miniband formation of Si nanodisc and its application in intermediate band photovoltaics. *Proc. of The 38th IEEE Photovoltaic Specialists Conference*, Austin Convention Center, Austin, Texas, 2012, 220 (4 pp.).
7. Luque, A.; Hegedus, S. *Handbook of Photovoltaic Science and Engineering*; John Wiley & Sons: UK, 2011.
8. Goldberg, D.E. *Genetic Algorithm in Search, Optimization and Machine Learning*; Addison-Wesley: New York, 1989.
9. Holland, J.H. *Adaptation in Natural and Artificial Systems: An Introductory Analysis with Applications to Biology, Control, and Artificial Intelligence*; MIT Press: Cambridge, 1992.
10. Li, Y.; Cho, Y.-Y. Intelligent BSIM4 model parameter extraction for sub-100 nm MOSFETs era. *Japanese Journal of Applied Physics* **2004**, *43*, 1717–1722.
11. Li, Y. Parallel genetic algorithm for intelligent model parameter extraction of metal-oxide-semiconductor field effect transistors. *Materials and Manufacturing Processes* **2009**, *24*, 243–249.
12. Li, Y. Hybrid intelligent approach for modeling and optimization of semiconductor devices and nanostructures. *Computational Material Science* **2009**, *45*, 41–51.
13. Li, Y.; Cho, Y.Y.; Wang, C.S.; Huang, K.Y. A genetic algorithm approach to InGaP/GaAs HBT parameters extraction and RF characterization. *Japanese Journal of Applied Physics* **2003**, *42*, 2371–2374.
14. Li, Y. An automatic parameter extraction technique for advanced CMOS device modeling using genetic algorithm. *Microelectronic Engineering* **2007**, *84*, 260–272.
15. Li, Y.; Yu, S.-M. A coupled-simulation-and-optimization approach to nanodevice fabrication with minimization of electrical characteristics fluctuation. *IEEE Transactions on Semiconductor Manufacturing* **2007**, *20*, 432–438.
16. Li, Y.; Cho, Y.-Y.; Wang, C.-S.; Huang, K.-Y. A genetic algorithm approach to InGaP/GaAs HBT parameter extraction and RF characterization. *Japanese Journal of Applied Physics* **2003**, *42*, 2371–2374.
17. Li, Y.; Yu, S.-M.; Li, Y.-L. Intelligent optical proximity correction using genetic algorithm with model- and rule-based approaches. *Computational Materials Science* **2009**, *45*, 65–76.
18. Paszkowicz, W. Genetic algorithms, a nature-inspired tool: Survey of applications in materials science and related fields. *Materials and Manufacturing Processes* **2009**, *24*, 174–197.

19. Chakraborti, N.; Das, S.; Jayakanth, R.; Pekoz, R.; Erkoç, Ş. Genetic algorithms applied to Li+ions contained in carbon nanotubes: An investigation using particle swarm optimization and differential evolution along with molecular dynamics. *Materials and Manufacturing Processes* **2007**, *22*, 562–569.
20. Li, Y.; Tseng, Y.-H. Differential evolutional approach to surface-potential-based model parameter extraction for nanoscale metal-oxide-semiconductor field effect transistors. *Materials and Manufacturing Processes* **2011**, *26*, 388–397.
21. Li, Y.; Cheng, H.-W.; Li, I.-H.; Yu, C.-H.; Lu, Z.-L. Electrical characteristic optimization of silicon solar cells using genetic algorithm. *Computer Methods in Materials Science* **2011**, *11*, 23–27.
22. Deb, K. *Multi-objective Optimization Using Evolutionary Algorithms*; John Wiley & Sons: West Sussex, UK, 2001.
23. Fonseca, C.M.; Fleming, P.J. Genetic algorithms for multiobjective optimization: Formulation, discussion and generalization. *Proc. of the Fifth International Conference on Genetic Algorithms* **1993**, 416–423.
24. Deb, K.; Agrawal, S.; Pratab, A.; Meyarivan, T. A fast elitist non-dominated sorting genetic algorithm for multiobjective optimization: NSGA-II. *Proc. of the Parallel Problem Solving from Nature VI Conference*, 2000, pp. 849–858.
25. Deb, K.; Pratap, A.; Agarwal, S.; Meyarivan, T. A fast and elitist multiobjective genetic algorithm: NSGA-II. *IEEE Transactions on Evolutionary Computation* **2002**, *6*, 182–197.
26. Knowles, J.D.; Corne, D.W. Approximating the nondominated front using the pareto archived evolution strategy. *Evolutionary Computation* **2002**, *8*, 149–172.
27. Biswas, A.; Maitre, O.; Mondal, D.N.; Das, S.K.; Sen, P.K.; Collet, P.; Chakraborti, N. Data-driven multiobjective analysis of manganese leaching from low grade sources using genetic algorithms, genetic programming, and other allied strategies. *Materials and Manufacturing Processes* **2011**, *26*, 415–430.
28. Li, Y.; Yu, S.-M.; Li, Y.-L. Electronic design automation using a unified optimization framework. *Mathematics and Computers in Simulation* **2008**, *79*, 1137–1152.
29. Li, Y.; Liu, J.-L.; Chao, T.-S.; Sze, S.M. A new parallel adaptive finite volume method for the numerical simulation of semiconductor devices. *Computer Physics Communications* **2001**, *142*, 285–289.
30. Li, Y.; Chao, T.-S.; Sze, S.M. A domain partition approach to parallel adaptive simulation of dynamic threshold voltage MOSFET. *Computer Physics Communications* **2002**, *147*, 697–701.
31. Li, Y.; Sze, S.M.; Chao, T.-S. A practical implementation of parallel dynamic load balancing for adaptive computing in VLSI device simulation. *Engineering with Computers* **2002**, *18*, 124–137.
32. Li, Y.; Yu, S.-M. A parallel adaptive finite volume method for nanoscale double-gate MOSFETs simulation. *Journal of Computational and Applied Mathematics* **2005**, *175*, 87–99.
33. Li, Y. A two-dimensional thin film transistor simulation using adaptive computing technique. *Applied Mathematics and Computation* **2007**, *184*, 73–85.
34. Juo, C.-F.; Liang, S.-W.; Tu, H.-M. Optimization parameters of femtosecond laser isolation processing for a microcrystalline silicon thin film solar cell. *Materials and Manufacturing Processes* **2011**, *26*, 1310.
35. Giri, B.K.; Hakanen, J.; Miettinen, K.; Chakraborti, N. Genetic programming through bi-objective genetic algorithms with a study of a simulated moving bed process involving multiple objectives. *Applied Soft Computing* **2013**, *13*, 2613–2623.
36. Mondal, D.N.; Sarangi, K.; Pettersson, F.; Sen, P.K.; Saxen, H.; Chakraborti, N. Cu-Zn separation by supported liquid membrane analyzed through Multi-objective Genetic Algorithms. *Hydrometallurgy* **2011**, *107*, 112.
37. Pettersson, F.; Chakraborti, N.; Saxen, H. A genetic algorithms based multi-objective neural net applied to noisy blast furnace data. *Applied Soft Computing* **2007**, *7*, 387.